

SenseComm: mmWave Tags for 5G-based Sensing

Swastik Kanjilal*

kanjis2@rpi.edu

Rensselaer Polytechnic Institute
Troy, New York, USA

Adithya Vijayan*

vijaya3@rpi.edu

Rensselaer Polytechnic Institute
Troy, New York, USA

Abstract

mmWave sensing remains reliable in fog, smoke, dust, and darkness, but detecting and *identifying* weak tag reflections in cluttered environments is difficult because direct-path and multipath components dominate the received signal. We design and study a retro-reflective mmWave fiducial tag (*Van Atta*-inspired) that modulates a low-rate bitstream using Gold-code spread-spectrum coding while reusing a 5G-style downlink OFDM waveform as the probing signal; the receiver applies clutter suppression via frequency shifting and correlation-based decoding. In OFDM simulations, the tag-modulated bit sequence is recovered reliably under favorable SNR, and introducing the tag increases the received reflected energy by up to 5.57 dB in our setup. These results support the feasibility of **OFDM-based coded retro-reflective tags** as practical radar-visible landmarks for integrated sensing and communication (ISAC), with clear next steps for controlled ON/OFF validation and phased-array hardware evaluation.

CCS Concepts

- Networks → *Network architectures*; • Hardware → *Beamforming*;
- Signal processing systems → *Radar signal processing*.

Keywords

mmWave sensing, retroreflective tags, Van Atta arrays, OFDM, backscatter, spread-spectrum coding, Gold codes, phased arrays, ISAC

1 Introduction

Millimeter-wave (mmWave) sensing is increasingly attractive for perception in conditions where optical sensors degrade—including fog, smoke, dust, low light, and glare. Operating at carrier frequencies on the order of 24–300 GHz, mmWave systems can leverage large bandwidths for fine range resolution and phased arrays for directional scanning. However, practical deployments in real environments remain limited by clutter and multipath: weak reflections of interest are often buried under strong direct-path components and uncontrolled environmental returns.

1.1 Motivation

Unlike cameras, mmWave sensors can maintain utility in visually adverse conditions. In addition, the wide bandwidths available at mmWave enable higher range resolution compared to many sub-6 GHz systems, and phased arrays provide angular selectivity through beam steering. These properties motivate using mmWave

not only for communication but also for robust sensing and localization in safety-critical settings.

1.2 Problem Statement

The central challenge is to reliably extract tag-induced information in high-clutter environments. In our setting, the tag-modulated return can be orders of magnitude weaker than the direct path and ambient reflections. As a result, the receiver must (i) suppress or compensate dominant components, (ii) isolate the tag response in frequency and/or code domains, and (iii) decode the tag’s embedded bits with high confidence under realistic impairments (noise, multipath, and hardware nonidealities).

1.3 Prior Work

Prior work has demonstrated the value of retro-reflective mmWave tags for robust detection and identification. For example, *R-Fiducial* introduces radar-visible markers based on retro-reflective architectures and code modulation to provide distinct signatures under FMCW radars. In parallel, systems such as *Millimetro* explore low-cost retro-reflective designs for long-range detection and precise localization. Inspired by these efforts, our work focuses on adapting the tagging and decoding principles to an *OFDM* setting, with the goal of reusing communication waveforms for sensing and tag readout.

1.4 Key Ideas

Our approach combines standard mmWave sensing primitives with spread-spectrum coding:

- **Range and angle processing:** range FFT and angle FFT (beamspace) to localize dominant scatterers.
- **Code-domain separability:** Gold-code modulation at the tag and correlation at the receiver to enable robust bit recovery.
- **Clutter mitigation:** frequency shifting (and corresponding downconversion) to separate tag energy from clutter concentrated near baseband.

This report studies a radar-friendly mmWave fiducial tag that aims to make infrastructure (e.g., signs or markers) intentionally detectable and identifiable to mmWave receivers while reusing communication-style waveforms. Specifically, we explore an OFDM-based pipeline in which a retro-reflective tag encodes a low-rate bitstream using spread-spectrum sequences (Gold codes), and the receiver performs correlation-based decoding to recover the tag data and improve separability from clutter.

We demonstrate (i) basic range/angle detection using a 24 GHz radar platform, and (ii) proof-of-concept recovery of tag-modulated bits in an OFDM simulation pipeline using Gold-code correlation

*Both authors contributed equally to this research.

and frequency shifting to reduce clutter sensitivity. We also outline a two-phase experimental plan: component-level validation of ON/OFF tag behavior (e.g., reflected power or RCS contrast) and system-level evaluation using phased-array OFDM hardware.

1.5 Contributions

- We propose an OFDM-based mmWave fiducial-tag pipeline that combines retro-reflective tagging with Gold-code spread-spectrum modulation and correlation-based decoding to enable tag identification in cluttered environments.
- We demonstrate proof-of-concept results via (i) 24 GHz range/angle sensing experiments and (ii) OFDM simulations showing reliable recovery of tag-modulated bits, and we outline a two-phase experimental plan for component- and system-level validation on phased-array hardware.

2 Background

Our mmWave tag system falls under some key research areas: mmWave sensing and backscatter communication, which all falls under integrated communication and sensing (ISAC).

2.1 R-Fiducial

R-fiducial, written by Kshitiz Bansal (University of California San Diego), Manideep Dunna (University of California San Diego), Sanjeev Anthia Ganesh (UCSD), Eamon Patamasing (UCSD), and Dinesh Bharadia (UCSD), heavily influenced our work, and helped with our methodology. Their R-fiducial tags help radars accurately identify and locate objects in low visibility environments. Their tags utilize Van-Atta architecture, and also contain/use gold code spread spectrum coding to give the tags their own unique signatures.

In the end, their tags were able to accurately identify objects indoor and outdoor with 100 percent accuracy up to 25 meters and 120 degree field of vision (FoV).

2.2 Millimetro

Similar to R-fiducial, Millimetro also discusses their work in Van-Atta retroreflective tags. They introduce more low cost tags, compared to R-fiducial: more of an emphasis on compact and simplicity. Additionally, they achieve 100 meters of range, with centimeter accurate ranging, for both indoor and outdoor environments. Their research has applications in various fields such as autonomous driving and robotics.

3 Design

We have both software and hardware elements to our system

3.1 Hardware

We first started on a software called CstStudio. Here, we developed a standard patch antenna operating at 5.6 GHz, giving us a great S11 reflection of around -38 dB.

The length and width of this singular patch antenna was 4.938 mm x 2.475 mm. Then we increased the operating frequency to 12 GHz and inspected whether we can still produce a good dB. We got an S11 reflection of -29.8, which is still a good simulation.

Finally, we increased up to 27GHz. In this final simulation we got an S11 reflection of -19.26 dB, which is still good.

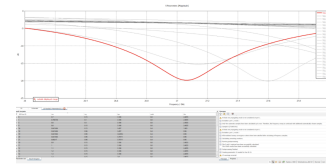


Figure 1: 27 GHz S11 Reflection

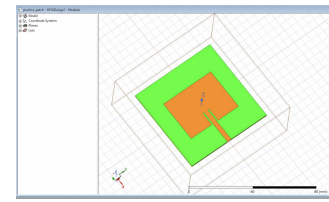


Figure 2: 27GHz Patch Antenna

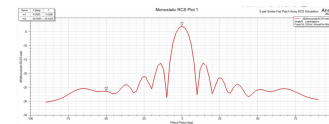


Figure 3: Monostatic RCS Plot

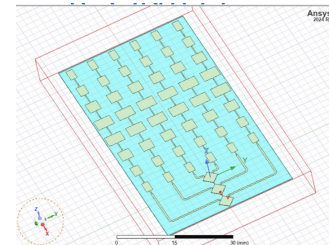


Figure 4: Van-Atta Architecture on HFSS

Moving forward, we moved onto a new software: HFSS. Here we had the model of our Van-Atta architecture at 24 GHz. What is Van-Atta architecture? Van-Atta architecture is an antenna design that reflects signals directly back to where they came from, which we call retro reflectivity. The symmetric elements of the architecture are connected by equal length transmission lines. Currently, we are working towards getting an acceptable RCS (radial cross section) plot, before enhancing to 28 GHz.

Another major component of the Van-Atta architecture is the switch. In this iteration of the design, we used a switch from MACOM called 011102 (Fig. 5). This shows the 3 major pins: RFC, RF1, and RF2. RFC is always connected to the receiver. This is due to the fact that signals will always be incoming to the tag, so the receiver needs to be connected at all times. RF1 is connected to the transmitter, and RF2 is connected to ground. This allows the switch to modulate between 1s and 0s.

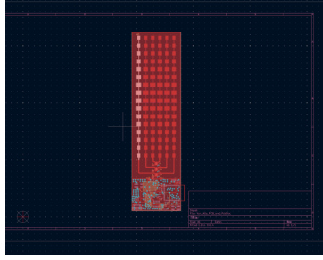


Figure 5: Van-Atta Architecture

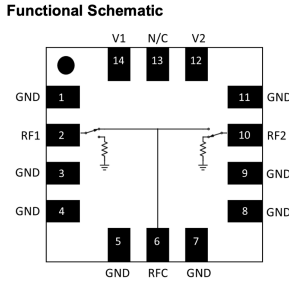


Figure 6: MACOM Switch Schematic

3.2 Software

Firstly, our system simulation works by having our transmitter and receiver placed next to each other due to the tag's retro reflective properties. On the transmitter side, we generate an OFDM signal with parameters $N = 64$ subcarriers and $CP = 16$. The signal is sent to the tag which modulates its data bits with the gold code. What is a gold code? Gold codes are binary sequences that map bit 1 to $+1$ and bit 0 to -1 . This allows for reduced interference with other signals. Then we do frequency shifting, so that we can separate from the clutter centered around 0 Hz. Then at the receiver, we take the total signal, subtract out the direct signal, and divide by the direct signal.

$$\text{Tag} = (\text{Total} - \text{Direct}) / \text{Direct}$$

Then, we multiply by the frequency shifting again, bringing the signal back down to baseband frequencies.

$$\text{DemodulatedSignal} = \text{Tag} * \cos(2\pi f_m t)$$

Finally, we multiply by the gold code again and summing the bits up, to achieve high peaks and low troughs, allowing us to see the high and low correlation values, giving us the data bits that the tag wanted to send.

4 Evaluation

We will go through our implementation for the software and hardware used in our system.

4.1 Software and Parameters

Firstly, we used python to help run our simulations. Our sampling frequency was 20 MHz, and as mentioned previously our OFDM



Figure 7: Tag Data Bits Reconstruction

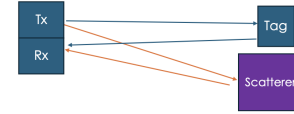


Figure 8: Setup

signal had 64 subcarriers and the cyclic prefix length was 16. Our modulation scheme can be changed, but we used 4-QAM or QPSK. Finally, our bit rate (tag switching) was 1ms.

How does the receiver determine our tag bits? As mentioned before, we multiply the gold code with our tag data bits at the tag. For example, this looks like if our data bit is 1, and our gold code is $[1, -1, 1, -1]$, our first "chunk" is $[1, -1, 1, -1]$. If our data bit is 0, and our gold code is the same of $[1, -1, 1, -1]$, we end up with $-1^*[1, -1, 1, -1] = [-1, 1, -1, 1]$. This is what is known as spread spectrum coding. At the end (the receiver), we multiply by the gold code again and sum. Therefore, taking what we had previously we do our first chunk of $[1, -1, 1, -1]$ multiplied with the gold code (which stays the same), which is $[1, -1, 1, -1]$. This results in $(1^*1) + (-1^*-1) + (1^*1) + (-1^*-1) = 1 + 1 + 1 + 1 = 4$. This is a positive correlation score, which correlates to bit 1. On the flip side, the second chunk is $[-1, 1, -1, 1]$, and this is multiplied by our same gold code ($[1, -1, 1, -1]$). When multiplied and summed we get $(-1^*1) + (1^*-1) + (-1^*1) + (1^*-1)$, which results in a correlation score of -4 (less than 0), which means it corresponds to bit 0 (Fig.6).

E.g., With $m = 5$ bit LFSRs $\rightarrow 31$ -bit Gold codes.

Capacity = $2^{m/2} = 2^{5/2} = 5.6$; Autocorrelation = $2^m - 1 = 31$ peaks

4.2 Baseline

Our only baseline comparison that we conducted was with no tag. In this case, we were able to see a normal QPSK constellation diagram. For future work, we will work on other baseline experiments to compare our system to. This will help us more determine what to change, and what to keep the same.

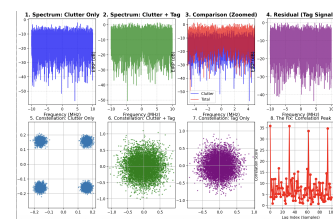


Figure 9: Addition of Tag in Environment

5 Analysis

As seen in Fig. 7, the data bits that the tag modulated (1, 0, 1, 0, 1, 0, 1, 0, 1, 0), are accurately recovered at the receiver. This, however, works best when SNR is high. Therefore, for future work, we need to look at this reproducibility when SNR is lower, and if we can still accurately determine the bits that we want from the tag.

Additionally, we see an increase of 5.57 dB when the tag is introduced into the system. This makes sense, as more of the signal is actually reflected back to the receiver in this environment because of the tag's retro-reflectivity.

6 Conclusion

This project demonstrates that a 5G-style downlink OFDM waveform can serve as a radar-like probe when paired with mmWave fiducial tags engineered to retro-reflect strongly and to encode information that the base station can reliably recover. Rather than introducing a new sensing waveform or deploying additional infrastructure, we leverage what already exists in modern cellular systems: wideband OFDM, beamforming, and the fact that a carefully designed tag can behave as a “radar-visible marker” in the environment.

On the signal-processing side, we validated the feasibility of spread-spectrum backscatter over OFDM using Gold-code modulation and correlation, together with frequency shifting to separate the tag response from dominant direct-path and clutter components. In simulation, the tag-modulated bit sequence is recovered accurately under favorable SNR, and the introduction of the tag produces a measurable increase in received reflected energy, consistent with the expected retro-reflective behavior. On the experimental side, early beam-sweep measurements qualitatively support the core premise: the tag appears as a distinct, strong lobe under directional scanning—exactly the type of high-confidence landmark needed when cameras and optical fiducials fail (e.g., fog, darkness, dust, or smoke).

The main takeaway is that we are not merely detecting objects; we are making infrastructure intentionally detectable and identifiable to mmWave systems using a lightweight tag that aligns naturally with existing OFDM hardware. Going forward, the most important next steps are: (i) rigorous tag ON/OFF validation (via RCS or reflected-power contrast in controlled horn measurements), (ii) robust decoding at lower SNR and in multipath, and (iii) system-level evaluation on phased-array hardware where real impairments (CFO, phase noise, beam quantization, and synchronization limits) must be handled explicitly. If these components are validated end-to-end, these tags offer a practical route toward radar-visible “traffic signs” for ISAC: high-reliability landmarks that can be detected and decoded even when vision-based systems are effectively blind.

7 Future Work

7.1 Phase I: Tag and Switch Validation

The first stage focuses on verifying that the mmWave tag behaves as designed and that the RF switches can reliably toggle between the intended reflection states.

7.1.1 Measurement Setup. We employ a bistatic configuration with two horn antennas:



Figure 10: Bistatic Setup

- One horn operates as the transmit antenna, illuminating the tag.
- The second horn serves as the receive antenna, capturing the field scattered by the tag.
- The tag is mounted on a low-reflection support (e.g., RF absorber or low-RCS foam) at a fixed distance from both horns.
- Measurements are performed in an anechoic chamber or a sufficiently absorptive environment to minimize multipath.

A DC power supply is used to bias the tag switches. In the absence of the microcontroller, the ON state is enforced using the design bias $V_1 = -5\text{ V}$ and $V_2 = 0\text{ V}$. An OFF state is defined by removing the bias (e.g., both control lines at 0 V, or as specified by the switch design).

Depending on the available instrumentation, the scattering is characterized either by:

- a vector network analyzer (VNA) measuring S_{21} between the two horns, or
- a radar front-end or power detector measuring the received power at the receive horn.

7.1.2 RCS / Reflected Power Measurement Procedure.

(1) System calibration (no tag):

- Place no object (or only a minimal fixture) at the tag location.
- Measure the baseline link (S_{21} or received power) over the frequency band of interest.
- Use this as the background reference.

(2) Reference target measurement (optional):

- Place a known metal plate with similar size to the tag at the same position.
- Measure S_{21} or received power versus frequency (and angle, if angular sweeps are performed).
- Use this as a reference for approximate calibration of the absolute or relative RCS of the tag.

(3) Tag in OFF state:

- Mount the tag at the reference position.
- Set the control voltages to the OFF bias condition (no or minimal bias).
- Record S_{21} (or received power) across the frequency range around the design frequency.
- Optionally, sweep the azimuth angle by rotating the tag/horns to obtain RCS.

(4) Tag in ON state:

- Apply the ON bias ($V_1 = -5\text{ V}$, $V_2 = 0\text{ V}$).

- Repeat the same set of measurements (frequency sweep, angular sweep).
 - Compare ON and OFF responses to confirm that the switches produce the expected change in reflection level and pattern.
- (5) **RCS estimation or EIRP-based assessment:**
- If full gain and distance calibration is available, convert the measured data to monostatic or bistatic RCS using standard radar equations.
 - If this is not feasible, report:
 - relative reflected power (ON vs. OFF vs. metal plate) as a function of aspect angle, or
 - the equivalent isotropically radiated power (EIRP) of the reflected signal as a practical proxy for RCS.
 - The primary goal is to verify that the tag exhibits a strong, controllable reflection and that the measured response qualitatively matches the simulated RCS signature (frequency dependence, main-lobe direction, and ON/OFF contrast).

Once the ON/OFF contrast and overall reflection behavior are validated, we proceed to the system-level experiments.

7.2 Phase II: System-Level Evaluation with Phased Arrays and OFDM

After confirming that the tag and its switches operate correctly, we move to a system-level evaluation using a phased-array testbed and OFDM waveforms.

7.2.1 Simulation Dataset. We first generate a simulation dataset that mimics the 5G-style sensing scenario:

- Synthetic channels are created at multiple frequencies and tag locations, consistent with the phased-array geometry and operating band.
- For each configuration, we model:
 - direct clutter paths,
 - tag-reflected paths with the designed RCS and phase response, and
 - the OFDM waveform structure.
- The resulting dataset is split into training and evaluation sets for algorithm development and performance assessment.

This provides a controllable environment to validate the signal processing pipeline (e.g., clutter suppression, correlation with tag codes, localization) before moving to hardware.

7.2.2 Real-World Dataset and IBM Phased-Array Testbed. We then construct a real-world dataset using phased-array testbeds in the Ka-band (around 28 GHz) and the IBM phased array antenna module (PAAM):

- The setup consists of:
 - two SDR-based testbeds operating near 28 GHz, and
 - two IBM PAAM with an 8×8 phased array and 0.5λ element spacing.
- The PAAM provides fine-grained beam steering with 6-bit phase resolution, enabling flexible beam pattern generation and rapid beam scanning.

- The baseband OFDM signal is generated and processed using USRP SDRs:
 - a USRP B210 handles baseband signal generation and reception in some configurations, and
 - a USRP X310 is used to drive the PAAM.
- The PAAM and X310 are tightly synchronized using a 10 MHz reference clock and a PPS signal drawn from the USRP X310, enabling beam switching on the order of $10 \mu s$.
- The UE side is emulated by a PlutoSDR in a quasi-omnidirectional mode, transmitting an OFDM waveform to mimic a small handheld device.

7.2.3 Tag Evaluation with OFDM Beams. In the final experimental configuration:

- One IBM phased array (or phased-array front-end) acts as the transmitter, sending OFDM beams into the scene.
- A second phased array (or sensing front-end) acts as the receiver, collecting the signal after it has:
 - propagated through the environment,
 - reflected off the mmWave tag under test, and
 - been contaminated by clutter and noise.
- The tag is placed at controlled positions and orientations within the field of view of the array, and measurements are taken:
 - with the tag OFF and ON, and
 - over different beam directions and, if needed, different ranges.

The received baseband data (complex I/Q samples) are processed using the same pipeline as in simulation:

- array steering and calibration,
- clutter suppression,
- correlation with the tag's Gold code, and
- detection and localization of the tag path.

By comparing simulated and measured results, we can:

- quantify how closely the real system follows the EM and system-level models,
- evaluate the robustness of OFDM-based tag detection under realistic hardware impairments and multipath, and
- refine both the tag design and the signal processing to improve detection performance.

We will first work on improving decoding in lower SNR environments. Even further, we need to remove just the simulation environment and test the codes in a real-world system. In addition, we also want to try a multi-tag environment to simulate the receiver receiving multiple signals from multiple tags with different gold codes.

Furthermore, we are also working on enhancing our system to work at 28GHz.

Another part we did is that we ordered new switches: MACOM-011105. We did this because the original switches we ordered have a logic 1 at -5V and logic 0 at 0V, while the control part of the board work at positive voltages, so we now ordered a switch that also works at these voltages.

In summary, the experimental plan proceeds in two stages: (i) component-level validation of the tag and its switches using horn antennas and controlled biasing, and (ii) system-level validation in

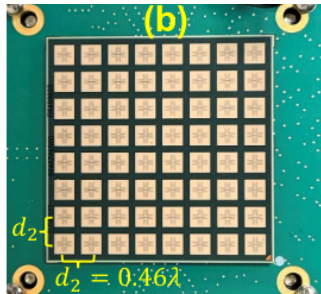


Figure 11: IBM Arrays



Figure 12: Outdoor Demonstration

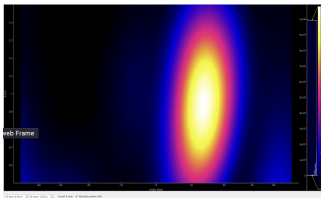


Figure 13: Demonstration Shown on Computer

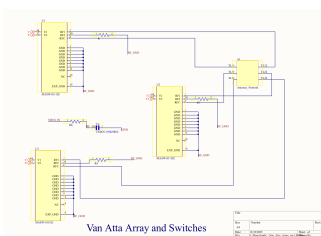


Figure 14: Switches and Array

a phased-array OFDM testbed with IBM PAAM and SDRs, using both simulated and real datasets to evaluate tag detectability and to compare simulation predictions with experimental measurements.

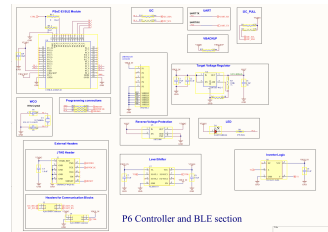


Figure 15: Controller Section

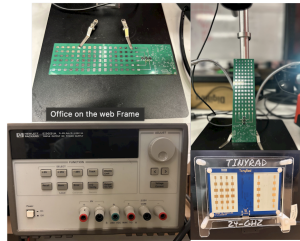


Figure 16: Components Used

8 Acknowledgment

We would like to acknowledge all the people who helped us with our system. We would first like to acknowledge Professor Jain for always being willing to help us through any of our challenges. Additionally, we would like to acknowledge Curtis Sung, who helped us with the HFSS simulation testing, soldering, and more. Next, we would like to acknowledge Nagarjun Bhat, who was willing to meet with us weekly to help answer any of our questions. Finally, we would like to acknowledge the authors of R-Fiducial, who inspired our project, and were also willing to help us with any questions we may have had.

9 References

References

- [1] M. Dunna, K. Bansal, S. A. Ganesh, E. Patamasing, and D. Bharadvia, "R-fiducial: Reliable and scalable radar fiducials for smart mmWave sensing," in *Proc. IEEE Vehicular Technology Conference (VTC)*, 2023.
- [2] E. Sharp and M. Diab, "Van Atta reflector array," *IRE Transactions on Antennas and Propagation*, vol. 8, no. 4, pp. 436–438, 1960.
- [3] R. Gold, "Optimal binary sequences for spread spectrum multiplexing," *IEEE Transactions on Information Theory*, vol. 13, no. 4, pp. 619–621, 1967.
- [4] K. M. Bae, N. Ahn, Y. Chae, P. Pathak, S.-M. Sohn, and S. M. Kim, "OmniScatter: Extreme sensitivity mmWave backscattering using commodity FMCW radar," in *Proc. ACM MobiSys*, 2022, pp. 316–329.
- [5] M. H. Mazaheri, A. Chen, and O. Abari, "mmTag: A millimeter wave backscatter network," in *Proc. ACM SIGCOMM*, 2021, pp. 463–474.
- [6] S. Lee, J. Park, K. Kim, R. N. Watson, and K. Chang, "Millimetro: mmWave retro-reflective tags for accurate, long range localization," in *Proc. ACM MobiSys*, 2021.
- [7] S. Cho, Y. Wang, P. Pathak, and U. Madhow, "Toward spoofing-resilient and communication-integrated mmWave radar sensing," in *Proc. ACM MobiSys*, 2021.
- [8] X. Zhang, Z. Yang, M. Li, and K. Tan, "SuperSight: Sub-cm NLOS localization for mmWave backscatter," in *Proc. ACM MobiCom*, 2022.
- [9] H. Chae, J. Park, Y. Lee, S. Han, and D. Wetherall, "mmComb: High-speed mmWave commodity WiFi backscatter," in *Proc. USENIX NSDI*, 2024.

Received Course report for ECSE 6560 (MCS), Fall 2025, Rensselaer Polytechnic Institute. Instructor: Prof. Ish Jain.